Dual-mode electromagnetically induced transparency and slow light in a terahertz metamaterial

Kun Zhang, Cheng Wang, Ling Qin, Ru-Wen Peng,* Di-Hu Xu, Xiang Xiong, and Mu Wang

National Laboratory of Solid State Microstructures and Department of Physics, Nanjing University, Nanjing 210093, China

**Corresponding author: rwpeng@nju.edu.cn*

Received March 10, 2014; revised May 1, 2014; accepted May 1, 2014;
posted May 5, 2014 (Doc. ID 207869); published June 9, 2014

In this Letter, we construct a metamaterial with dual-mode electromagnetically induced transparency (EIT)-like behavior by introducing "bright atoms," "quasi-dark atoms," and "dark atoms" simultaneously. The dual-mode EIT-like behavior has been demonstrated both experimentally and theoretically in terahertz (THz) regime. At two EIT-like modes, slow light is also observed as two time-delayed wave packets, and the effective group refractive index can reach 10^2. Furthermore, stable dual-mode EIT-like behavior is verified in this metamaterial for a wide range of oblique incident angles. Our work provides a design approach to mimic dual-mode EIT, and such an approach may achieve potential applications on miniaturized and versatile THz devices.

OCIS codes: (160.3918) Metamaterials; (040.2235) Far infrared or terahertz; (230.4555) Coupled resonators; (060.4230) Multiplexing.

http://dx.doi.org/10.1364/OL.39.003539

Electromagnetically induced transparency (EIT) is a coherent process observed in three-level atomic systems, and it makes an absorptive media transparent to the probe field, simultaneously accompanied by slow group velocity [1,2]. However, it requires complicated experimental conditions, since the coherence time in the atomic system is rather short. It becomes easier to exhibit EIT-like behavior in the systems consisting of coupled mechanical or electrical resonators [3], which have attracted much attention to classical analogs of EIT. In recent years, with the development of metamaterials [4], a variety of EIT metamaterials have been reported at microwave [5–7], terahertz (THz)[8–10], near-infrared [11–16], and optical regions [17–19], and some of which are even tunable and quite useful in designing active devices [20–23]. However, most structures in previous works only possess a single EIT-like mode, which may limit applications on miniaturized and versatile devices. Very recently, interest has been extended to dual or multiple EIT-like modes via inductive coupling [24,25], Fabry–Perot resonators [26], or exciting magnetic dipoles by breaking the symmetry [27].

In this Letter, we offer a different theoretical approach to achieve dual-mode EIT in a metamaterial, and then demonstrate it experimentally in THz regime. As we know, a significant difference in the quality factors of the two resonances should be required to develop EIT-like phenomenon. Therefore, we can easily construct two different EIT-like systems by respectively introducing a "dark atom" [17] or "quasi-dark atom" [8] to couple with the "bright atom". We find that, by introducing these three meta-atoms simultaneously, it exhibits dual-mode EIT-like behavior, which is nonexistent in three-level atomic systems in nature.

Let us start with a system consisting of two electric dipoles P_1 and P_2, both of which have the same resonant frequency ω_0 and couples with the incident field E_0. The dynamic equation of the system can be described as linearly coupled Lorentzian oscillators as follow [3]:

$$\begin{cases} \ddot{P}_1(t) + \gamma_1 \dot{P}_1(t) + \omega_0^2 P_1(t) - \Omega^2 P_2(t) = \kappa_1 E_0(t) \\ \ddot{P}_2(t) + \gamma_2 \dot{P}_2(t) + \omega_0^2 P_2(t) - \Omega^2 P_1(t) = \kappa_2 E_0(t) \end{cases}, \quad (1)$$

where γ_1 and γ_2 are the damping factors of the dipoles, κ_1 and κ_2 are the coupling coefficients between the dipoles and the incident field, and Ω is the coupling coefficient between the dipoles. Based on Eq. (1), we can obtain the susceptibility determined by $\chi_E = P_1/E_0$. Under the second-order approximation, we get the following susceptibility, depending on the coupling coefficients κ_1 and κ_2:

$$\chi_E = \kappa_1 \left[\frac{(\gamma_2^2\omega^2 - \Omega^4)(\omega_0^2 - \omega^2)}{(\gamma_1\gamma_2\omega^2 + \Omega^4)^2} + i \frac{\gamma_2 \omega}{\gamma_1\gamma_2\omega^2 + \Omega^4} \right] - \kappa_2 \left[\frac{\Omega^2}{\gamma_1\gamma_2\omega^2 + \Omega^4} + i \frac{(\gamma_1 + \gamma_2)\Omega^2(\omega_0^2 - \omega^2)\omega}{(\gamma_1\gamma_2\omega^2 + \Omega^4)^2} \right]. \quad (2)$$

For $\kappa_2 = 0$, the system consists of a "bright atom" and a "dark atom," as described in Fig. 1(a), and its susceptibility in Fig. 1(d) shows a transparent window around ω_0, i.e., single-mode EIT-like behavior. For $0 < \kappa_2 < \kappa_1$, as schematically shown in Fig. 1(b), the "dark atom" is replaced by a "quasi-dark atom," which couples with

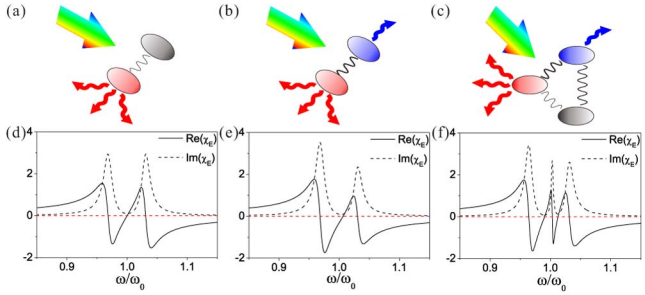

Fig. 1. (a) Schematic of the system consisting of a "bright atom" and a "dark atom," and (d) shows its susceptibility. (b) System consisting of a "bright atom" and a "quasi-dark atom," and (e) shows its susceptibility. (c) System consisting of a "bright atom," a "dark atom," and a "quasi-dark atom," and (f) shows the susceptibility in this three-"atom" system.

the incident field weakly. Just as described in Fig. 1(e), EIT is also mimicked due to the coupling between a "bright atom" and a "quasi-dark atom".

Now, we consider a meta-molecule, as schematically described in Fig. 1(c), consisting of a "bright atom" (P_a), a "quasi-dark atom" (P_b), and a "dark atom" (P_c). Similar to Eq. (1), the dynamic equations follow:

$$\begin{pmatrix} P_a \\ P_b \\ P_c \end{pmatrix} = \begin{pmatrix} \omega_0^2 - \omega^2 - i\gamma_1\omega & -\Omega_{12}^2 & -\Omega_{13}^2 \\ -\Omega_{21}^2 & \omega_0^2 - \omega^2 - i\gamma_2\omega & -\Omega_{23}^2 \\ -\Omega_{31}^2 & -\Omega_{32}^2 & \omega_0^2 - \omega^2 - i\gamma_3\omega \end{pmatrix}^{-1} \times \begin{pmatrix} \kappa_1 E_0 \\ \kappa_2 E_0 \\ 0 \end{pmatrix}. \quad (3)$$

The susceptibility of such a system can be given by $\chi_E = P_a/E_0$, which also depends on the coupling coefficients κ_1 and κ_2. Here we set the coupling coefficients $\kappa_2 = 0.1\kappa_1$. The calculated susceptibility indicates two transparent windows around the resonant frequency (ω_0) [Fig. 1(f)]. Therefore, the dual-mode EIT-like effect can be achieved in this system with three coupled meta-atoms. It also offers a possibility to mimic multi-mode EIT by simultaneously introducing quasi-dark meta-atoms with different κ into one system. According to previous conclusions, it is easy to design a metamaterial consisting of three fundamental meta-atoms to exhibit dual-mode EIT-like behavior.

To verify the considerations above, we turn to a specific design of proper artificial atoms. Figure 2(a) shows the geometry of the designed "bright atom" under polarized incident light and its simulated transmission coefficient spectrum. The green shade shows the wide full width at half-maximum (FWHM), indicating a low quality factor. Then, we design a split-ring resonator (SRR), as described in Fig. 2(b), to act as a "dark atom." Under the normalized incident light, only the symmetric mode can be excited for the electric field polarized along the y direction [Fig. 2(d)], whereas the asymmetric mode is a dark mode; therefore, such a meta-atom can act as a "dark atom" for x-polarized illumination. In addition, we employ another kind of SRR [Fig. 2(c)] as a "quasi-dark atom." The transmission coefficient of such a SRR shows narrower FWHM and a larger quality factor, implying that this SRR couples with the incident field much more weakly than the "bright atom," therefore acting as a "quasi-dark atom." By varying the spatial dimensions of these three meta-atoms, we tune their resonant frequencies to the desired band around $\omega_0 = 0.66$ THz. We use the commercial finite-difference time-domain (FDTD) software package (Lumerical FDTD Solutions) to carry out all the simulations. The aluminum structures, with the same thicknesses of 4 μm, are arranged on a germanium substrate with a period of 96 μm. Based on the meta-atoms described above, we first construct two kinds of single-mode EIT-like metamaterials. One consists of "bright" meta-atoms and "dark" meta-atoms [Fig. 2(e)], and the other consists of "bright" meta-atoms and "quasi-dark" meta-atoms [Fig. 2(h)]. The

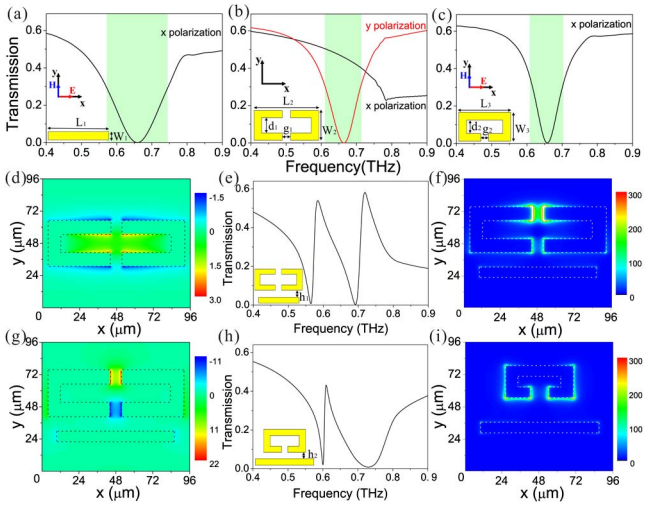

Fig. 2. Calculated transmission coefficient spectra in designed meta-atom systems: (a) the "bright atom," with $L_1 = 76$ μm and $W_1 = 8$ μm; (b) the "dark atom," with $L_2 = 88$ μm, $W_2 = 34$ μm, $d_1 = 14$ μm, and $g_1 = 8$ μm; and (c) the "quasi-dark atom," with $L_3 = 44$ μm, $W_3 = 24$ μm, $d_2 = 8$ μm, and $g_2 = 12$ μm. (d) Electric field distribution of the "dark atom" at 0.66 THz, with the electric field polarized along the y axis. (e) Transmission coefficient spectrum of system consisting of a "bright atom" and a "dark atom," with $h_1 = 11$ μm; (f) its electric field intensity distribution; (g) its electric field distribution (both at 0.58 THz). (h) Transmission coefficient spectrum of system consisting of a "bright atom" and a "quasi-dark atom," with $h_2 = 10$ μm; and (i) shows its electric field intensity distribution at 0.61 THz.

transmission coefficient spectra both have a transparency window, in accordance with the previous numerical calculations [Figs. 1(d) and 1(e)]. To present the intrinsic process, we pay attention to the field distribution at the resonant frequency. Figure 2(g) shows the electric field distribution with phase information of the structure in Fig. 2(e), indicating that the asymmetric mode of the "dark atom" is now excited in this EIT configuration. For the electric field intensity distributions of these two systems at the transparency windows [Figs. 2(f) and 2(i)], the "bright atom" is suppressed, and the "dark atom," or the "quasi-dark atom," is excited. The electromagnetic field is coupled between the "bright atom" and "dark (or quasi-dark) atom," leading to a destructive interference.

To achieve the dual-mode EIT-like effect, we combine the three meta-atoms to acquire the new "molecule" described in Fig. 3(a). The transmission spectrum [Fig. 3(b)] illustrates two transparency windows on the broad absorption background, i.e., a dual-mode EIT-like effect. In our design, both the distances between the meta-atoms and the orientation of the "quasi-dark atom" would affect the coupling coefficients between the dipoles. We find it can exhibit obvious dual-mode EIT-like behavior when the open end of the "quasi-dark atom" faces away from the "bright atom" with proper distances. To have a detailed insight of the dual-mode EIT-like behavior, we probe the field intensity distributions at the transparency windows, around $\omega_L = 0.565$ THz [Fig. 3(c)] and $\omega_H = 0.685$ THz [Fig. 3(d)], respectively. At these two frequencies, the "bright atom" is suppressed. Differently, at $\omega_L = 0.565$ THz [Fig. 3(c)], the "dark

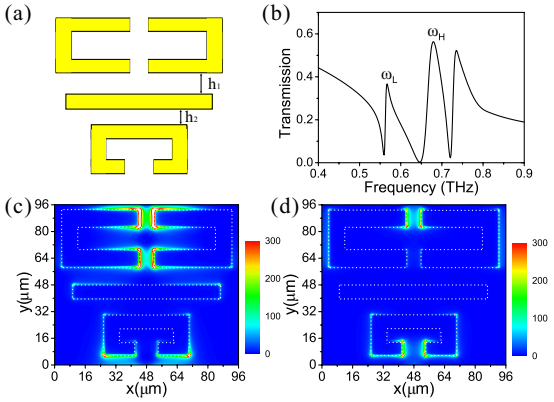

Fig. 3. (a) Schematic of meta-molecule with three meta-atoms, $h_1 = 11$ μm and $h_2 = 10$ μm. (b) Transmission coefficient spectrum of the metamaterial. (c), (d) Electric field intensity distributions at 0.565 and 0.685 THz, respectively.

atom" is greatly excited and the electric field is mainly localized around the two free ends of the "dark atom," similar to the field distribution of a dipole. In Fig. 3(d), at $\omega_H = 0.685$ THz, the electric fields around the "dark atom" and the "quasi-dark atom" are comparable. In addition, the electric field is localized around the free end of the "quasi-dark atom" and the further free end of the "dark atom," also similar to a dipole. In such a system, the field coupling back and forth among the three "atoms" and the two transparency windows both come from the destructive interference of the three "atoms".

Experimentally, the samples for THz waves were fabricated by photolithograph technique. Figure 4(a) shows one of micrographs of our samples, where the 1 μm-thick aluminum microstructure was deposited on a germanium substrate. Except the thickness, all other geometrical parameters are the same as those used in the simulation. Please note that, in the simulations, the thickness of metamaterials is set as 4 μm to increase the calculation accuracy; however, it is hard to fabricate such thick structures, so we adjust the sample thickness to be 1 μm in the experiments. Due to the fact that the skin depth of aluminum is about 300 nm in THz regime, such adjustment does not influence the physical effect.

The measurements are carried out with an Ekspla THz real-time spectrometer [Fig. 4(b)], with samples in a nitrogen purging box to keep a stable environment. The femtosecond laser beam is equally split into two beams: one act as a reference light and the other transmits through the samples. By scanning the delay line, the time-domain signals $E(t)$ of the polychromatic THz pulse transmitted through the sample [Fig. 4(a)] at normal incidence are illustrated in Fig. 4(c). Further, by carrying out Fourier-transformation on the experimental time-domain data, the transmission coefficient spectrum of the three-"atom" system [solid black curve in Fig. 4(d)] is achieved. For comparison, the experimental transmission coefficient spectrum of the bi-"atom" system [shown in Fig. 2(e)] is also given [dashed magenta curve in Fig. 4(d)]. It is obvious that two transparency windows appear around $\omega_1 = 0.56$ THz and $\omega_2 = 0.65$ THz for the three-"atom" system, whereas there is only a single transparency window for the bi-"atom" system. The observed phenomena agree reasonably with the simu-

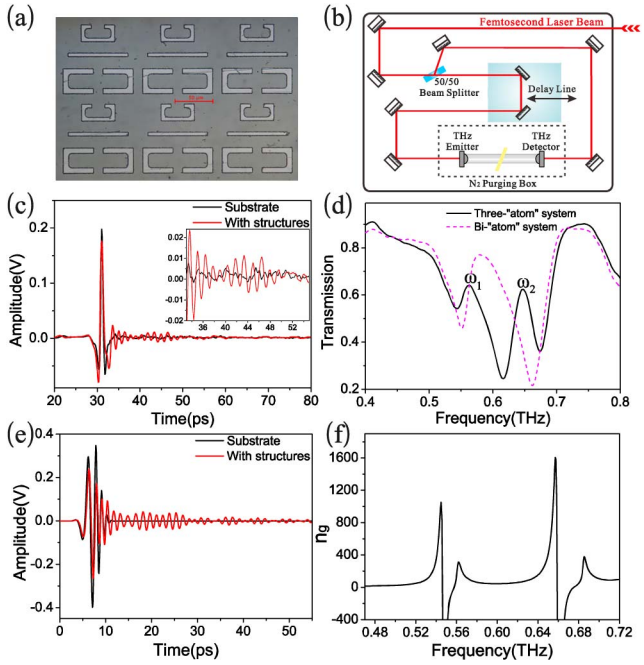

Fig. 4. (a) Micrograph of the three-"atom" system. (b) Diagram of the THz time-domain spectrometer. (c) Experimentally measured time-domain transmission signals of bare substrate (black curve) and sample with the three-"atom" system (red curve). The inset is an enlarged spectrum. (d) Experimental transmission spectra of the three-"atom" system (solid black curve) and the bi-"atom" system (dashed magenta curve). (e) Simulated time-domain transmission spectrum of the three-"atom" system. (f) Effective group refractive index retrieved from the simulated results in (e).

lated ones presented in Figs. 3(b) and 2(e). There yet exists some declination, mainly coming from geometrical deviation when fabricating the aluminum microstructures. Therefore, the dual-mode EIT-like effect has been achieved experimentally.

It is worth mentioning that the present metamaterial can slow light accompanying the dual-mode EIT-like effect. Two delayed wave packets have been demonstrated in both measured [in the inset of Fig. 4(c)] and simulated [Fig. 4(e)] time-domain spectra. Besides, the slow light effect can also be characterized by the group refractive index of the metamaterials. Based on the method in [28], we have retrieved the effective refractive index and then calculated the effective group refractive index via $n_g = n + \omega dn/d\omega$. As we can see in Fig. 4(f), the effective group refractive index reaches $n_g = 246.9$ at 0.565 THz, and $n_g = 377.0$ at 0.685 THz, which are comparably large for applications in THz devices. Comparing these two effective group refractive indices, we find $246.9:377.0 \approx 11:16.8$, matching with the ratio of the two-delay time in simulation, i.e., 11 ps : 17 ps. Therefore, both the time-delay and group refractive index verify that the THz waves can be slowed by the metamaterial. Our experimental observation in THz regimes with two-wave packets provides a direct evidence of the dual-mode behavior and slow light effect.

Finally, we pay attention to the dual-mode EIT effect in the present metamaterial for oblique incident waves. As shown in Figure 5, the light is incident with angle θ while

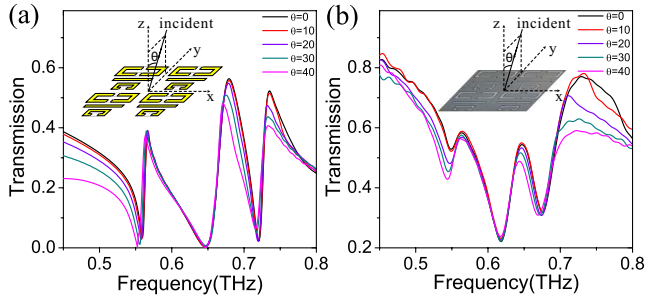

Fig. 5. Transmission coefficient spectra under oblique incident light with different incident angles (θ) (a) simulated and (b) experimental.

the electric field is parallel to the x axis. Figures 5(a) and 5(b) are simulated and experimental transmission spectra, respectively. With increasing the incident angle θ, the transparency windows have a slight redshift and the transmission becomes weaker. However, for the second transparency window around high frequencies, the redshift and amplitude change are more obvious. This can be explained by the dipole-like electric field distributions around the transparent windows, as shown in Figs. 3(c) and 3(d). For the first transparency window [Fig. 3(c)], only the "dark atom" is greatly excited. In addition, the "dark atom" is symmetric along the x direction; therefore, the first transparency window is not sensitive to such oblique incident light. However, for the second transparency window [Fig. 3(d)], the "quasi-dark atom" is also greatly excited, and is asymmetric along the x direction. Therefore, as the oblique incident angle changes, both the amplitude and the resonant frequency would change. Nevertheless, the dual-mode EIT-like behavior is still obvious and stable for a wide range of oblique incident angles. Therefore, by combining active elements (e.g., see [22]), such a system may serve as an optical logic gate, potentially leading to complete optical circuits on miniature circuit boards.

In summary, we have provided a different approach to achieve the metamaterials with dual-mode EIT-like behavior by introducing three kinds of artificial atoms into a system. The dual-mode EIT-like behavior has been demonstrated by analytical calculations, numerical simulations, and experimental measurements. At two EIT-like modes, slow light effects are also observed as two time-delayed wave packets, and the effective group refractive index can reach 10^2. Moreover, dual-mode EIT-like behavior in the metamaterial is kept for a wide range of oblique incident angles. Under the design discipline we put forward, dual-mode EIT can be mimicked in various structural shapes, and multi-mode behavior is also possible. Our work provides a way to control and manipulate THz waves and may achieve potential applications on integrated THz devices.

This work has been supported by the Ministry of Science and Technology of China (Grant Nos. 2012CB921502 and 2010CB630705) and the National Natural Science Foundation of China (Grant Nos. 11034005, 11204127, 11321063, and 91321312).

References

1. S. E. Harris, J. E. Field, and A. Imamoglu, Phys. Rev. Lett. **64**, 1107 (1990).
2. M. Fleischhauer, A. Imamoglu, and J. P. Marangos, Rev. Mod. Phys. **77**, 633 (2005).
3. C. L. G. Alzar, M. A. G. Martinez, and P. Nussenzveig, Am. J. Phys. **70**, 37 (2002).
4. Y. M. Liu and X. Zhang, Chem. Soc. Rev. **40**, 2494 (2011).
5. N. Papasimakis, V. A. Fedotov, N. I. Zheludev, and S. L. Prosvirnin, Phys. Rev. Lett. **101**, 253903 (2008).
6. Y. Sun, H. Jiang, Y. Yang, Y. Zhang, H. Chen, and S. Zhu, Phys. Rev. B **83**, 195140 (2011).
7. P. Tassin, L. Zhang, R. Zhao, A. Jain, T. Koschny, and C. M. Soukoulis, Phys. Rev. Lett. **109**, 187401 (2012).
8. S. Y. Chiam, R. Singh, C. Rockstuhl, F. Lederer, W. Zhang, and A. A. Bettiol, Phys. Rev. B **80**, 153103 (2009).
9. L. Qin, K. Zhang, R. W. Peng, X. Xiong, W. Zhang, X. R. Huang, and M. Wang, Phys. Rev. B **87**, 125136 (2013).
10. F. Zhang, Q. Zhao, J. Zhou, and S. Wang, Opt. Express **21**, 19675 (2013).
11. P. Tassin, L. Zhang, T. Koschny, E. N. Economou, and C. M. Soukoulis, Phys. Rev. Lett. **102**, 053901 (2009).
12. C. Y. Chen, I. W. Un, N. H. Tai, and T. J. Yen, Opt. Express **17**, 15372 (2009).
13. J. Zhang, S. Xiao, C. Jeppesen, A. Kristensen, and N. A. Mortensen, Opt. Express **18**, 17187 (2010).
14. S. D. Liu, Z. Yang, R. P. Liu, and X. Y. Li, Opt. Express **19**, 15363 (2011).
15. J. Chen, P. Wang, C. Chen, Y. Lu, H. Ming, and Q. Zhan, Opt. Express **19**, 5970 (2011).
16. Z. Ye, S. Zhang, Y. Wang, Y. Park, T. Zentgraf, G. Bartal, X. Yin, and X. Zhang, Phys. Rev. B **86**, 155148 (2012).
17. S. Zhang, D. A. Genov, Y. Wang, M. Liu, and X. Zhang, Phys. Rev. Lett. **101**, 047401 (2008).
18. N. Liu, L. Langguth, T. Weiss, J. Kastel, M. Fleischhauer, T. Pfau, and H. Giessen, Nat. Mater. **8**, 758 (2009).
19. N. Verellen, Y. Sonnefraud, H. Sobhani, F. Hao, V. V. Moshchalkov, P. Van Dorpe, P. Nordlander, and S. A. Maier, Nano Lett. **9**, 1663 (2009).
20. Y. Lu, J. Y. Rhee, W. H. Jang, and Y. P. Lee, Opt. Express **18**, 20912 (2010).
21. L. Verslegers, Z. Yu, Z. Ruan, P. B. Catrysse, and S. Fan, Phys. Rev. Lett. **108**, 083902 (2012).
22. J. Gu, R. Singh, X. Liu, X. Zhang, Y. Ma, S. Zhang, S. A. Maier, Z. Tian, A. K. Azad, H. Chen, A. J. Taylor, J. Han, and W. Zhang, Nat. Commun. **3**, 1151 (2012).
23. W. Cao, R. Singh, C. Zhang, J. Han, M. Tonouchi, and W. Zhang, Appl. Phys. Lett. **103**, 101106 (2013).
24. J. Kim, R. Soref, and W. R. Buchwald, Opt. Express **18**, 17997 (2010).
25. L. Zhu, F. Y. Meng, J. H. Fu, Q. Wu, and J. Hua, Opt. Express **20**, 4494 (2012).
26. J. Chen, C. Wang, R. Zhang, and J. Xiao, Opt. Lett. **37**, 5133 (2012).
27. C. Kurter, P. Tassin, L. Zhang, T. Koschny, A. P. Zhuravel, A. V. Ustinov, S. M. Anlage, and C. M. Soukoulis, Phys. Rev. Lett. **107**, 043901 (2011).
28. D. R. Smith, S. Schultz, P. Markos, and C. M. Soukoulis, Phys. Rev. B **65**, 195104 (2002).